# Fault diagnosis of rolling element bearing based on the empirical wavelet transform technique and correlation coefficient

Abdelgawad H.A. Mattar[a,*], Hussien Sayed[a], Younes K. Younes[a], Heba H. El-Mongy[a, b]

[a] *Department of Mechanical Design, Faculty of Engineering- Mataria, Helwan University, Egypt.*

[b] *Centre for Applied Dynamics Research, School of Engineering, University of Aberdeen, UK.*

## Abstract

Several time-frequency analysis methods have been applied to the detection and diagnosis of rolling-element bearing faults. One such method is the empirical wavelet transform (EWT), which is used for signal analysis. This study combines the EWT method with the correlation coefficient to diagnose bearing faults using experimentally measured vibration signals. First, the empirical wavelet transform method is used to analyze the vibration signal and extract the amplitude modulated-frequency modulated (AM-FM) modes. Subsequently, the correlation coefficient is computed to identify significant components that indicate bearing faults. Finally, the envelope spectrum is generated for these significant components in order to extract the characteristic frequencies associated with bearing faults. The findings demonstrate the effectiveness of this novel approach in accurately identifying bearing fault characteristics.

**Keywords:** Rolling-element bearings; Fault diagnosis; Empirical wavelet transform; Correlation coefficient; Signal processing.

## Introduction

Rolling-element bearings are crucial and commonly used machine components in rotating equipment [1]. Bearing damage can result from problems in the manufacturing process or errors during assembly, but it can also happen when the bearing is subjected to difficult working circumstances. The performance of the equipment is directly impacted by bearing defects, which can also result in production losses, shorter equipment lifespans, or even catastrophic failures [2-5]. As a result, early detection of these defects without machine disassembly is critical for

condition monitoring, quality inspection, and predictive maintenance. Several reviews have surveyed the development of approaches for early detection and diagnosis of bearing problems throughout the last decades [6-9].

Empirical wavelet transform (EWT) is a novel technique that was created by Gilles [10]**.** The vibration signal produced by defective bearings can be described as a complex modulation signal, in which the impulsive frequency of the faulty bearings varies due to the modulation of the bearing resonance frequency and/or the rotational frequency of the shaft. Therefore, the use of EWT for bearing defect detection is appropriate. Liu and Chen [11] provided a broad summary of the developments in the study of the EWT method and its applications in machine fault diagnosis.

Kedadouche et al. [12] used a numerically generated signal to assess EWT, empirical mode decomposition (EMD), and ensemble empirical mode decomposition (EEMD). The results showed that the EWT is better than the EEMD and EMD in mode estimates, and computation time is significantly reduced. El-Mongy [13] combined the parameter-less empirical wavelet transform (PEWT) with envelope detection (ED). The results suggested that the novel method extracted the bearing fault features successfully. Lopez et al. [14] suggested an empirical wavelet transform (EWT)-based methodology for detecting bearing faults. The experimental results revealed that the proposed technique efficient in diagnosing induction motor-bearing defects. To extract the bearing fault characteristics, Hu et al. [15] proposed an enhanced empirical wavelet transform (EEWT) technique for bearing detection. Both theoretical and practical findings showed that the suggested technique is noise resistant and accurate for detecting bearing faults. The results showed that the proposed technique has high prediction accuracy. Xin et al. [16] suggested a novel fault diagnostic method based on reinforced empirical Morlet wavelet transform (REMWT) for overcoming the drawbacks of classic EWT in rotating machinery fault diagnosis. Xue et al. [17] suggested an approach that combines enhanced empirical wavelet transform (EEWT) with correlation kurtosis (CK). The findings revealed that the suggested approach was better than that of the classic EWT. Xu et al. [18] developed a frequency band multidivisional and overlapped based on EWT technique to accurately determine the highest component of kurtosis. They found that the suggested method has good accuracy and effectiveness. Huang et al. [19] introduced a new technique based on frequency phase space

empirical wavelet transform (FPSEWT). The results showed that the suggested approach can successfully extract rolling element bearing defect characteristics.

This paper provides a rolling bearing defect diagnostic method based on the use of EWT for defective bearings experimental signals for the purpose of fault feature extraction. Some improvements will also be made to the EWT technique in order to overcome its limitations.

**Fundamental Theory of the Empirical Wavelet Transform**

Gilles [10] gave the theoretical details about the empirical wavelet transform. EWT is a new approach to building adaptive wavelets. Assume that the Fourier spectrum of a real valued signal $f(t)$ falls within the range $[0,\pi]$. Finding the local maxima in the spectrum and sorting them in decreasing order is the first stage in segmenting a spectrum confined from 0 to $\pi$ into $N$ contiguous segments. Then, the boundaries of all segments are denoted by $\omega_n$ (where $\omega_0$=0 and $\omega_N$= $\pi$ . Thus, the midway between any two successive maxima is the definition of a segment. The symbol for each section is $\Lambda_n$= $[\omega_{n-1},\omega_n]$. Hence, it can be seen that $\cup_{n=1}^{N} \Lambda_n = [0,\pi]$. A transient phase of width $2\tau_n$is defined for each $\omega_n$ , where $\tau_n$ is assumed to be proportional to $\omega_n$ (Where $\Upsilon = \tau_n/\omega_n$) and $0 < \Upsilon < 1$. $\Upsilon$ Is the proportion between the cutoff frequency and the transition bandwidth, and it may be selected in accordance with the following requirement:

$$\Upsilon < \min\left(\frac{\omega_{n+1} - \omega_n}{\omega_{n+1} + \omega_n}\right) \tag{1}$$

The band-pass filters on each segment are how the empirical wavelets are defined. It is decided to use the Meyer wavelet as the foundation wavelet function. In Equations (2) and (3), the empirical scaling function and the empirical wavelets are respectively shown.

$$\hat{\varphi}_n(\omega) = \begin{cases} 1 & \begin{cases} \text{if } |\omega| \le \omega_n - \tau_n \\ \text{if } \omega_n - \tau_n \le |\omega| \le \omega_n + \tau_n \end{cases} \\ \cos\left[\frac{\pi}{2}\beta\left(\frac{1}{2\tau_n}(|\omega| - \omega_n + \tau_n)\right)\right] & \\ 0 & \text{Otherwise} \end{cases} \tag{2}$$

$$\hat{\Psi}_n(\omega) = \begin{cases} 1 & \text{if } \omega_n + \tau_n \le |\omega| \le \omega_{n-1} + \tau_{n-1} \\ \cos\left[\frac{\pi}{2}\beta\left(\frac{1}{2\tau_{n-1}}(|\omega| - \omega_{n+1} + \tau_{n+1})\right)\right] & \text{if } \omega_{n+1} - \tau_{n+1} \le |\omega| \le \omega_{n+1} + \tau_{n+1} \\ \sin\left[\frac{\pi}{2}\beta\left(\frac{1}{2\tau_n}(|\omega| - \omega_n + \tau_n)\right)\right] & \text{if } \omega_n - \tau_n \le |\omega| \le \omega_n + \tau_n \\ 0 & \text{Otherwise} \end{cases} \tag{3}$$

Where the $\beta(x)$ is an arbitrary function in $C^k$ ([0, 1]) such that.

$$\beta(x) = \begin{cases} 0 & if\ x \le 0 \\ , and\ \beta(x) + \beta(1-x) = 1\ \forall x \in [0,1] & \\ 1 & if\ x \ge 1 \end{cases} \quad (4)$$

Numerous polynomial functions meet these requirements. The classic example of this function is represented by the following polynomial, which was initially proposed by Daubechies [20] and utilized by Gilles [10] as well as in this study, the standard example of this function is

$$\beta(x) = x^4(35 - 84x - 70x^2 - 30x^3) \quad (5)$$

The empirical wavelet transform can be defined in the same way as the traditional wavelet transform. The inner product of the signal *f (t)* with the scaling function $\phi_1$ yields the approximation coefficients $W_f^{\varepsilon}(0, t)$.

$$W_f^{\varepsilon}(0,t) = \langle f, \phi_1 \rangle = \int f(\tau)\overline{\phi_1(\tau - t)}\, d\tau = IFFT(\overline{\hat{f}(\omega) * \widehat{\phi_1}(\boldsymbol{\omega})}) \quad (6)$$

The detail coefficients $W_f^{\varepsilon}(n, t)$ are the inner products of the signal and the empirical wavelets $\psi_n$:

$$W_f^{\varepsilon}(n,t) = \langle f, \quad \psi_n \rangle = \int f(\tau)\overline{\psi_n(\tau - t)}\, d\tau = IFFT(\overline{\hat{f}(\omega) * \widehat{\psi_n}(\boldsymbol{\omega})}) \quad (7)$$

The IFFT symbolizes the inverse Fourier transform, while $f(\omega)$ denotes the Fourier transform of $f(t)$.

Consequently, the reconstructed signal may be calculated as follows:

$$\begin{aligned} f(t) &= W_f^{\varepsilon}(0,t) * \phi_1(t) + \sum_{n=1}^{N} W_f^{\varepsilon}(n,t) * \psi_n(t) \\ &= IFFT\left(\widehat{W_f^{\varepsilon}}(0,\omega)\right) * \widehat{\phi_1}(\boldsymbol{\omega}) + \sum_{n=1}^{N} \widehat{W_f^{\varepsilon}}(n,\omega) * \widehat{\psi_n}(t) \end{aligned} \quad (8)$$

Where the convolution is represented by $(*)$ the signal empirical modes may thus be expressed as follows:

$$\begin{aligned} f_0(t) &= W_f^{\varepsilon}(0,t) * \phi_1(t) \\ f_k(t) &= W_f^{\varepsilon}(k,t) * \psi_k(t) \end{aligned} \quad (9)$$

Gilles [21] suggested a segmentation technique based on scale space representation. A flowchart that depicts the suggested algorithm's whole process is shown in Fig. 1.

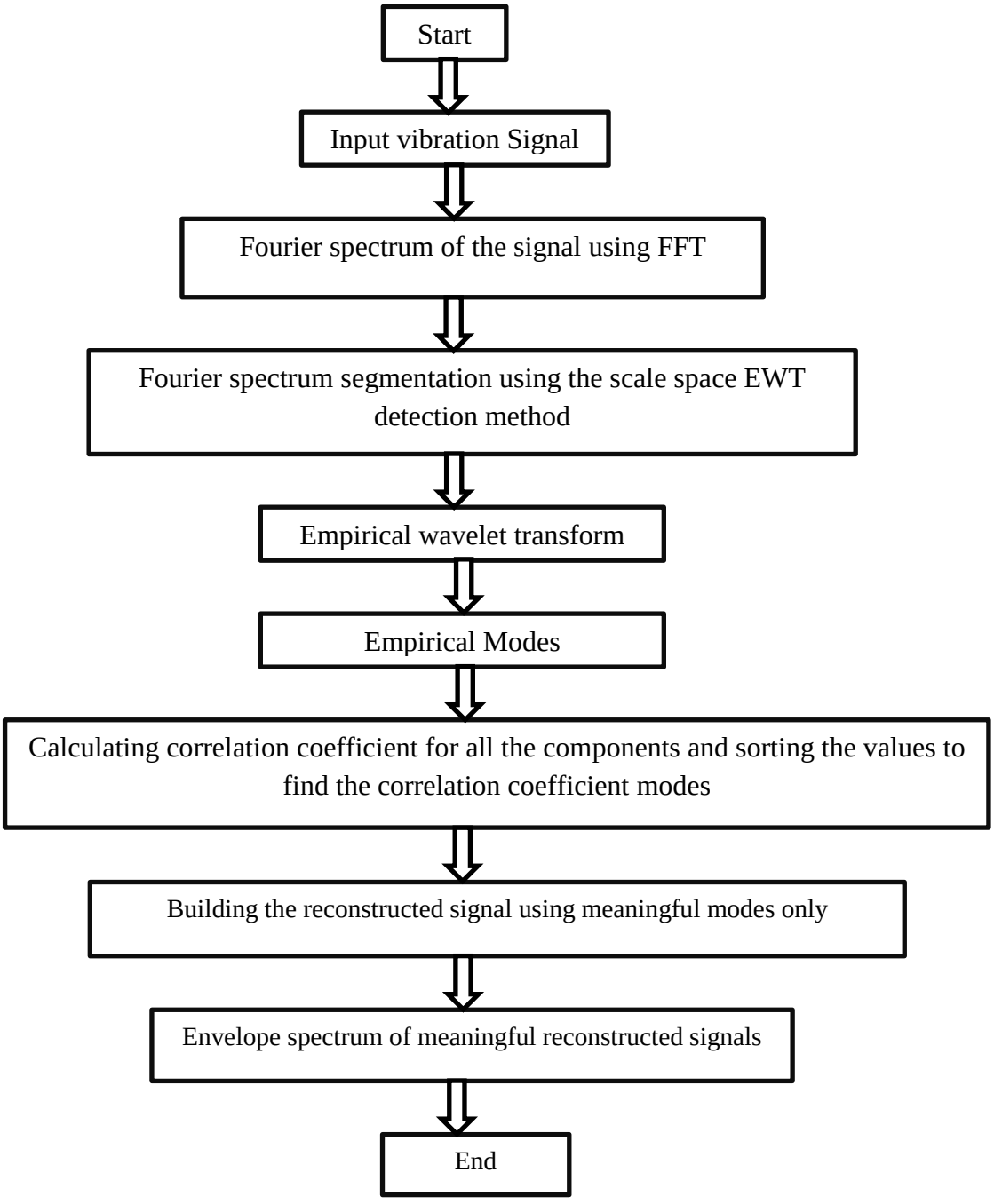


Fig.1. Flow chart of process of fault detection using empirical wavelet transforms.

**Experimental setup**

The fault demonstrator shown in Fig. 2, created by G.U.N.T., is utilized for conducting experiments on faulty bearings at shaft speed of 1500 rpm. The machinery fault demonstrator comprises a steel shaft equipped with a single disk positioned at its midpoint, secured by a taper lock mechanism. The shaft is supported by two deep groove ball bearings (SKF 6004) and is connected to an electric motor with a power output of 0.37 kW, through a jaw coupling. A total of 20,000 signal samples were collected at a sampling rate of 4000 Hz, Using accelerometers to measure both horizontal and vertical vibration signals.

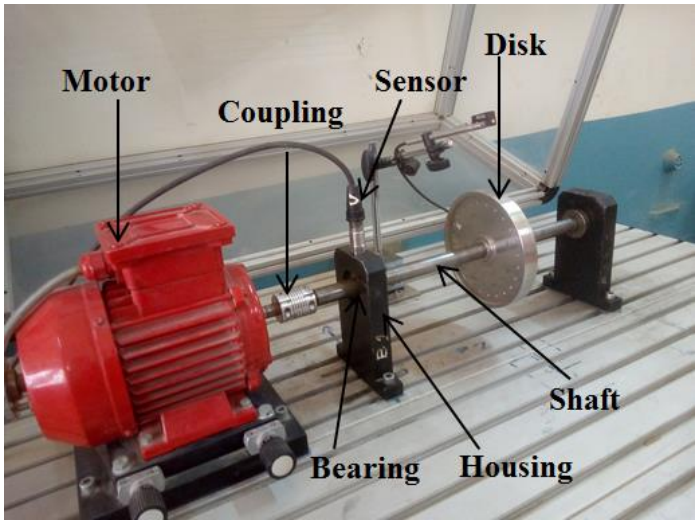


Fig.2: Machinery fault demonstrator made by G.U.N.T. [22]

**Results and discussion**

In this section, the experimental results are presented to assess the effectiveness of EWT in feature extraction of the bearing faults, namely, outer race defect.

**EWT results of outer race defect for experimental signal**

Fig. 3 (a) illustrates the measured time waveform on the bearing with outer race defect at the shaft rotational speed of 1500 rpm in horizontal direction. Fig. 3 (b) shows the segmentation of the Fourier spectrum of experimental vibration signal, using EWT scale space detection method.

The scale space automatically finds the meaningful modes in a spectrum. The EWT method's Fourier bounds are shown as dashed vertical lines.

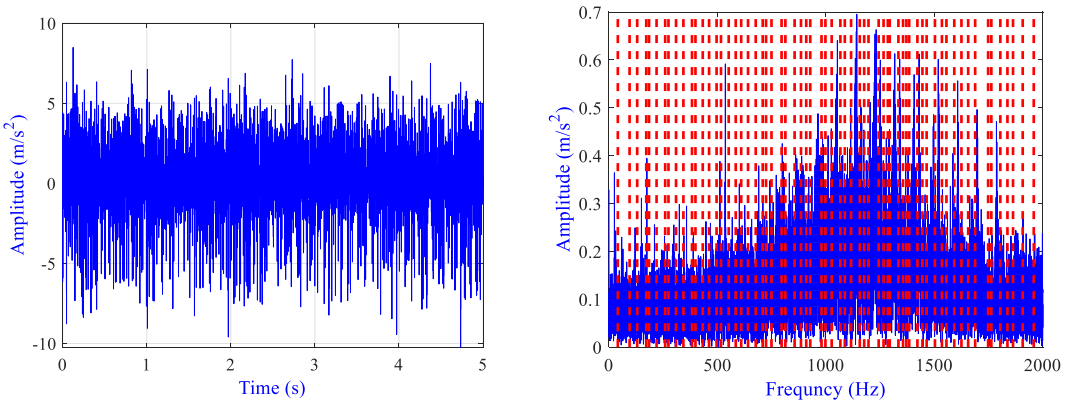


(a) (b)

Fig.3. Experimental vibration signal (outer race fault), (a) Time record, (b) segmented frequency spectrum using scale space EWT.

Fig. 4 shows the decomposition using the scale space EWT of experimental vibration signal. It can be seen in Fig. 4 that the EWT decomposed the experimental vibration signal into signals with different frequencies, which can be considered as different modes since they have different frequencies and energies. It is evident that EWT can efficiently decompose the signal and precisely separate components of various frequencies.

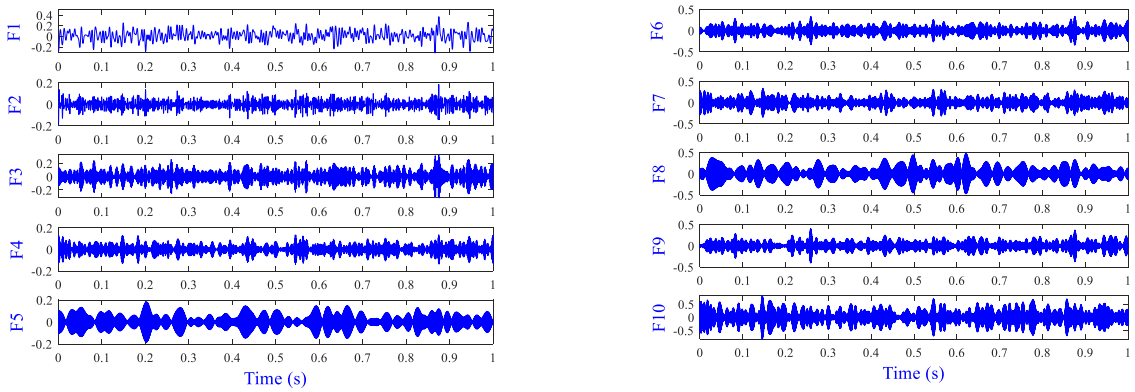


Fig.4. Experimental vibration signal decomposition using the scale space EWT (Continued)

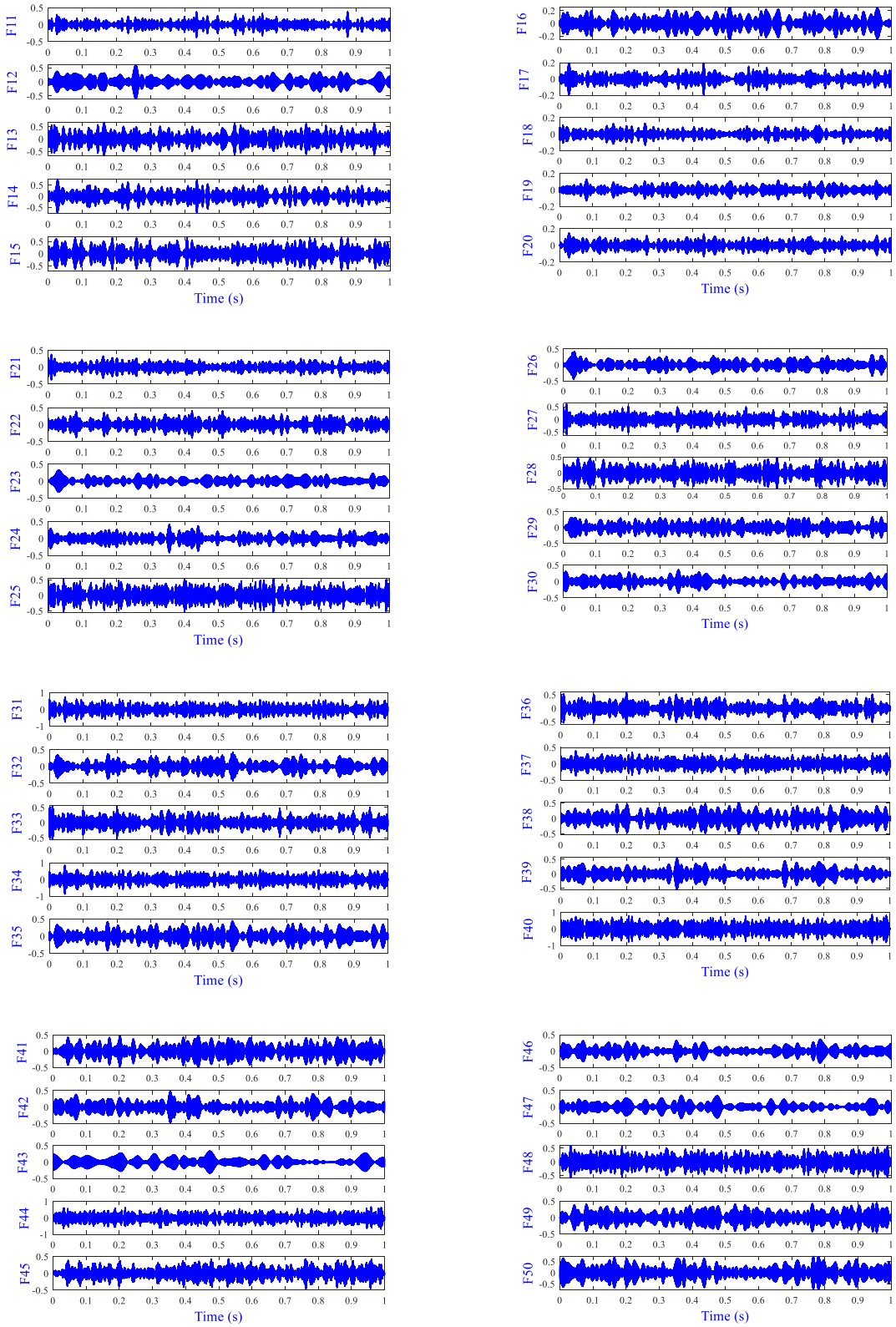


Fig.4. Experimental vibration signal decomposition using the scale space EWT (Continued)

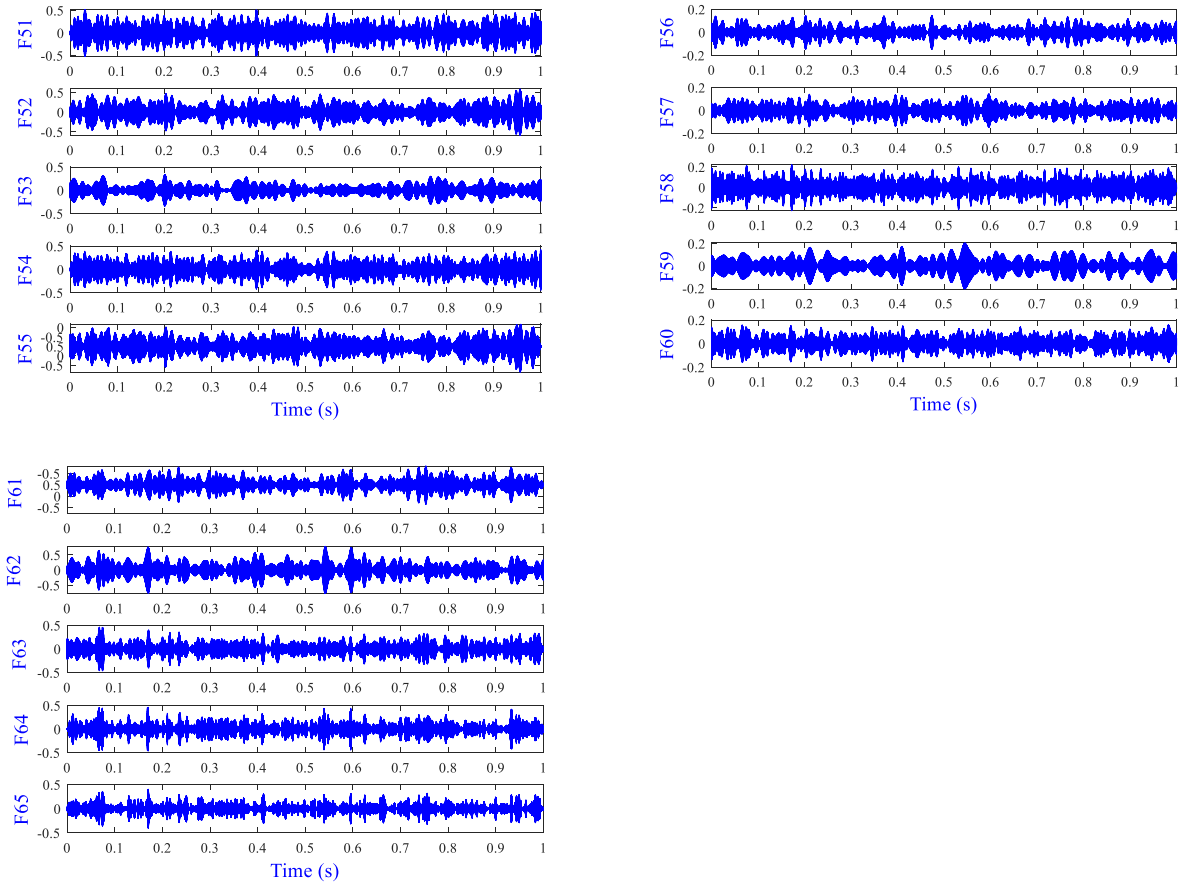


Fig.4. Experimental vibration signal decomposition using the scale space EWT

Fig. 5 showed the kurtosis value and correlation coefficient for all the EWT components. The obtained values are sorted in a descending order to identify the set of EWT modes with elevated kurtosis and correlation coefficient. The kurtosis and correlation coefficient values for EWT components having values that exceed a specific level are retained, while the others are removed. For the measured signal, the red dashed lines reflect this. The components F37, F40, and F44 are having high correlation coefficient, while the components F9, F11, and F64 are having high kurtosis value. Fig. 6 shows the meaningful modes and the reconstructed signal using the F37, F40, and F44 modes only. While Fig. 7 shows the meaningful modes and the reconstructed signal using the F9, F11, and F64 modes only.

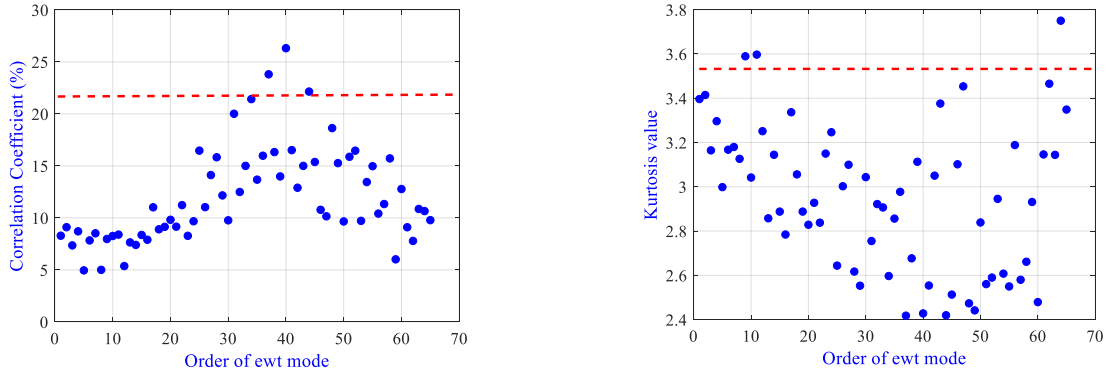


(a) (b)

Fig.5. Kurtosis values and correlation coefficient for EWT components of measured signal, (a) Kurtosis values, and (b) correlation coefficient

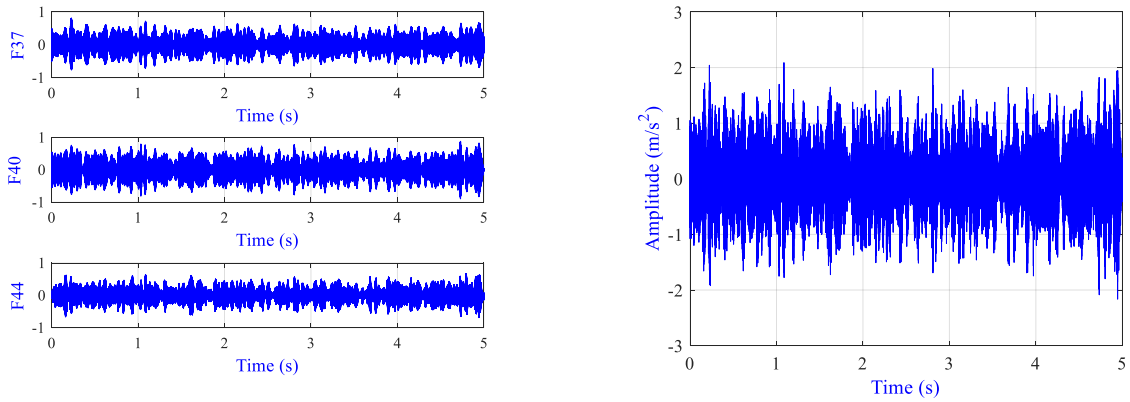


(a) (b)

Fig.6. Experimental vibration bearing fault signal, (a) Meaningful components having high correlation coefficient value, (b) Meaningful reconstructed signal

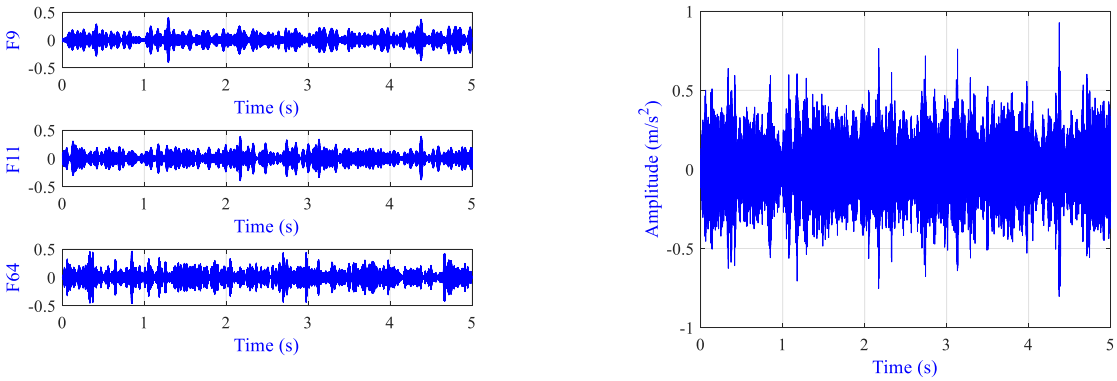


(a) (b)

Fig.7. Experimental vibration bearing fault signal, (a) Components having high kurtosis value, (b) Reconstructed signal

The envelope spectra of EWT components having elevated correlation coefficient are plotted in Fig.8 (a). The envelope spectrum shows the peaks at BPFO and a number of its harmonics. Therefore, the meaningful components having high correlation coefficient values can be selected as a suitable diagnostic feature in the analysis of the outer race defect. While the envelope spectra of EWT components have elevated kurtosis is plotted in Fig.8 (b). Fig.8 (b) shows a peak at BPFO only, so it can be inferred that the components having high kurtosis value were not enough to construct a meaningful signal that comprises all the features of the outer race fault.

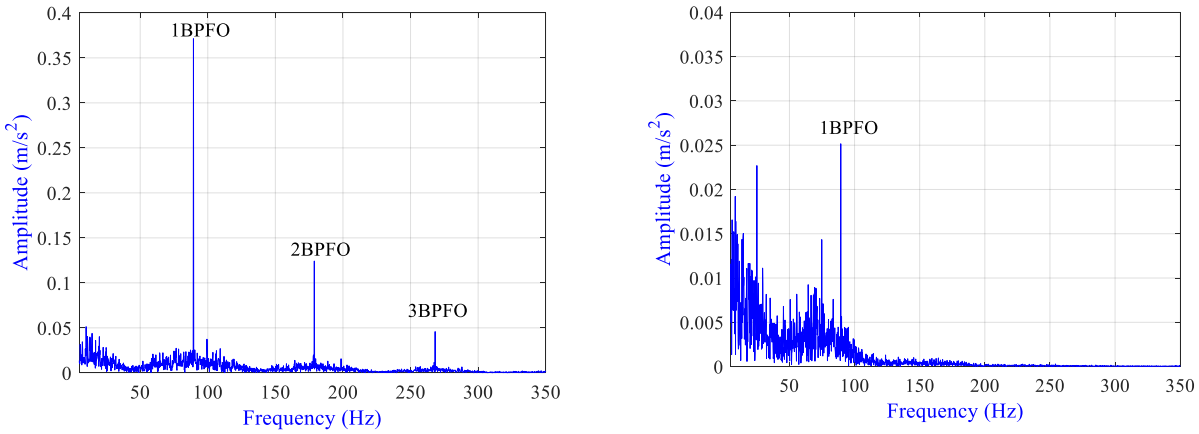


(a) (b)

Fig.8. Envelope spectrum of the meaningful reconstructed signal component, (a) EWT components having elevated correlation coefficient, and (b) EWT components have elevated kurtosis.

## Conclusions

This study explored the application of the Empirical Wavelet Transform (EWT) technique for bearing fault diagnosis. Experimental signals from a fault demonstrator provided by G.U.N.T. were utilized to evaluate the effectiveness of the EWT method. By employing the EWT-correlation coefficient procedure, a meaningful reconstructed signal was obtained. Afterwards, the envelope spectrum was used to show the bearing fault features. It was concluded that the correlation coefficient was more efficient in extracting the meaningful EWT modes that are relevant to the bearing fault in comparison with the kurtosis parameter. Overall, these findings confirmed the efficacy of the EWT approach for successful bearing fault diagnosis.

## References


1. Tiwari, R., *Rotor systems: analysis and identification*. 2017: CRC press.
2. Cheng, H., Y. Zhang, W. Lu, and Z. Yang, *Research on ball bearing model based on local defects.* SN Applied sciences, 2019. **1**(10): p. 1-10.
3. Kulkarni, S.S., A.K. Bewoor, and R.B. Ingle, *Vibration signature analysis of distributed defects in ball bearing using wavelet decomposition technique.* Noise & Vibration Worldwide, 2017. **48**(1-2): p. 7-18.
4. Kulkarni, S. and S.B. Wadkar, *Experimental investigation for distributed defects in ball bearing using vibration signature analysis.* Procedia Engineering, 2016. **144**: p. 781-789.
5. Karmakar, S., S. Chattopadhyay, M. Mitra, and S. Sengupta, *Induction motor fault diagnosis: approach through current signature analysis*. 2016: Springer.
6. Anwarsha, A. and T. Narendiranath Babu, *Recent advancements of signal processing and artificial intelligence in the fault detection of rolling element bearings: A review.* Journal of Vibroengineering, 2022. **24**(6): p. 1027-1055.
7. Abdelkader, R., A. Kaddour, and Z. Derouiche, *Enhancement of rolling bearing fault diagnosis based on improvement of empirical mode decomposition denoising method.* The International Journal of Advanced Manufacturing Technology, 2018. **97**(5): p. 3099-3117.
8. Feng, Z., Ming Liang, and Fulei Chu., *Recent advances in time–frequency analysis methods for machinery fault diagnosis: A review with application examples.* Mechanical Systems and Signal Processing, 2013. **38.1** p. 165-205.
9. Bauer, M., N. Balaratnam, J. Weidenauer, F. Wagner, and M. Kley, *Comparison of envelope demodulation methods in the analysis of rolling bearing damage.* Journal of Vibration and Control, 2022: p. 10775463221129155.
10. Gilles, J., *Empirical wavelet transform.* IEEE transactions on signal processing, 2013. **61**(16): p. 3999-4010.
11. Liu, W. and W. Chen, *Recent advancements in empirical wavelet transform and its applications.* IEEE Access, 2019. **7**: p. 103770-103780.
12. Kedadouche, M., M. Thomas, and A. Tahan, *A comparative study between Empirical Wavelet Transforms and Empirical Mode Decomposition Methods: Application to bearing defect diagnosis.* Mechanical Systems and Signal Processing, 2016. **81**: p. 88-107.
13. El-Mongy, H.H. *Feature extraction enhancement based on parameterless empirical wavelet transform: Application to bearing fault diagnosis*. Military Technical College.

14. Lopez-Gutierrez, R., J.d.J. Rangel-Magdaleno, C.J. Morales-Perez, and A. García-Perez, *Induction Machine Bearing Fault Detection Using Empirical Wavelet Transform.* Shock and Vibration, 2022. **2022**.
15. Hu, Y., X. Tu, F. Li, H. Li, and G. Meng, *An adaptive and tacholess order analysis method based on enhanced empirical wavelet transform for fault detection of bearings with varying speeds.* Journal of sound and vibration, 2017. **409**: p. 241-255.
16. Xin, Y., S. Li, Z. Zhang, Z. An, and J. Wang, *Adaptive reinforced empirical Morlet wavelet transform and its application in fault diagnosis of rotating machinery.* IEEE Access, 2019. **7**: p. 65150-65162.
17. Xue, J., H. Xu, X. Liu, D. Zhang, and Y. Xu, *Application of enhanced empirical wavelet transform and correlation kurtosis in bearing fault diagnosis.* Measurement Science and Technology, 2022. **34**(3): p. 035023.
18. Xu, Y., Z. Fan, K. Zhang, and C. Ma, *A novel method for extracting maximum kurtosis component and its applications in rolling bearing fault diagnosis.* Shock and Vibration, 2019.
19. Huang, X., G. Wen, L. Liang, Z. Zhang, and Y. Tan, *Frequency phase space empirical wavelet transform for rolling bearings fault diagnosis.* IEEE Access, 2019. **7**: p. 86306-86318.
20. Hu, Y., F. Li, H. Li, and C. Liu, *An enhanced empirical wavelet transform for noisy and non-stationary signal processing.* Digital Signal Processing, 2017. **60**: p. 220-229.
21. Gilles, J. and K. Heal, *A parameterless scale-space approach to find meaningful modes in histograms—Application to image and spectrum segmentation.* International Journal of Wavelets, Multiresolution and Information Processing, 2014. **12**(06): p. 1450044.
22. Mattar, A.H.A., H. Sayed, Y.K. Younes, and H.H. El-Mongy, *Experimental Verification and Nonlinear Dynamic Response Analysis of a Rolling Element Bearing with Localized Defects.* Journal of Failure Analysis and Prevention, 2022. **22**(4): p. 1753-1770.